

Haemodynamic simulation of aneurysm coiling in an anatomically accurate computational fluid dynamics model: technical note

Aristotelis P. Mitsos · Nikolaos M. P. Kakalis · Yiannis P. Ventikos · James V. Byrne

Received: 10 July 2007 / Accepted: 17 October 2007 / Published online: 28 November 2007
© Springer-Verlag 2007

Abstract

Introduction Computational fluid dynamics (CFD) is a numerical technique that is used for studying haemodynamic parameters in cerebral aneurysms. As it is now possible to represent an anatomically accurate intracranial aneurysm in a computational model, we have attempted to simulate its endosaccular occlusion with coils and demonstrate the haemodynamic changes induced. This is the first attempt to use this particular porous medium-based method for coiling simulation in a CFD model, to our knowledge. **Methods** Datasets from a rotational 3-D digital subtraction angiogram of a recently ruptured anterior communicating aneurysm were converted into a 3-D geometric model and the discretized data were processed using the computational technique developed. Coiling embolisation simulation was achieved by impediment of flow through a porous medium with characteristics following a series of embolisation coils.

Part of this work was the subject of the first author's thesis for his Master of Science in Interventional Neuroradiology (University of Oxford, 2006) and part of it was presented as an oral presentation at the European Society of Neuroradiology Symposium (ESNR 2006 - Geneva).

A. P. Mitsos (✉) · J. V. Byrne
Department of Neuroradiology, John Radcliffe Hospital,
University of Oxford,
Level 1 - West Wing, Headley Way, Headington,
Oxford OX3 9DU, United Kingdom
e-mail: aristotelis.mitsos@wolfson-oxford.com

N. M. P. Kakalis · Y. P. Ventikos
Department of Engineering Science, University of Oxford,
Parks Road,
Oxford OX1 3PJ, United Kingdom

A. P. Mitsos
Wolfson College, University of Oxford,
Linton Road,
Oxford OX2 6UD, United Kingdom

Haemodynamic parameters studied were: pressure distribution on the vessel wall, blood velocity and blood flow patterns.

Results Significant haemodynamic changes were detected after deployment of the first coil. Similar, but less dramatic changes occurred during subsequent stages of coiling. The blood flow patterns became less vortical in the aneurysm sac as velocity decreased to stagnation and the wall pressure at the fundus was gradually reduced. Furthermore, the haemodynamic characteristics developed at the area of the neck remnant could form the basis for assessing the likelihood of delayed coil compaction and aneurysm regrowth.

Conclusion Appropriate computational techniques show great promise in simulating the haemodynamic behaviour of the various stages in coil embolisation and may be a potentially valuable tool in interventional planning and procedural decision-making.

Keywords Computational fluid dynamics · Aneurysm model · Porous medium · Coiling · Technical note

Introduction

Computational fluid dynamics (CFD) is a numerical method for modelling haemodynamics, which has been applied to the study of intracranial aneurysms. Image-based simulations of blood flow dynamics have been reported in different types of cerebral aneurysms [1–3] and a number of haemodynamic parameters studied to understand the influence of flow on their natural history [4–7]. More recently, researchers have attempted to simulate the haemodynamic consequences of endovascular interventional procedures using data from clinical cases [8–11].

In this study, we used a novel computational method, based on CFD, to simulate the endovascular coil embolisation of a recently ruptured cerebral aneurysm in an anatomically accurate 3-D computer model representation derived from a clinical case. The method used to model the coiling process of this aneurysm involved simulation of a porous medium within the aneurysm and decreasing its porosity as coils are inserted. The characteristics of the porous medium were modelled on the coil chart used in clinical practice. Subsequently, the haemodynamic changes induced during the different stages of the coiling process were analysed, as well as the local haemodynamic conditions which develop following aneurysm occlusion with a residual neck remnant. To our knowledge, this is the first report of such a study.

Material and methods

Aneurysm realistic computer model

The clinical data used for modelling purposes were derived from a ruptured large and wide-necked bifurcation aneurysm (11×9.4×7.8 mm) arising from the anterior communicating artery (Fig. 1). A series of 15 GDC-10 detachable platinum coils (Boston Scientific, Target, Fremont, Calif.) were deployed (Table 1). A packing density of 26.5% (i.e. percentage of sac lumen occupied by metal) was simulated but leaving a small aneurysm remnant at the neck area to ensure unobstructed flow through both distal anterior cerebral arteries (Fig. 2). 3-D imaging data were obtained using a Siemens Axiom-Artis angiography system (Siemens Medical Solutions, Erlangen, Germany). 3-D subtraction angiography images were reconstituted from a rotational acquisition. The protocol used included a 200° spin over 6 s



Fig. 1 Left ICA digital subtraction angiogram showing the ruptured anterior communicating artery aneurysm

at 40°/s and imaging at 1.5°/s, followed by intraarterial injection of 15 ml of a nonionic iodinated contrast agent (Niopam 300 mg/ml, Nycomed, France) using an automatically triggered pump injection through a catheter positioned in the left internal carotid artery (ICA). The X-ray exposure parameters were: 70 kV, 155 mA, pulse width 10 ms and 1.20 μ Gy/pulse. A total of 150 mask and angiography images were acquired in 1,024² matrices and reconstituted on a Leonardo workstation (Siemens) for 3-D display. The anonymized datasets were processed using Amira 3.1 (Mercury Computer Systems, Chelmsford, Mass.), a visualization system able to represent 3-D aneurysm imaging data as a triangular surface and create volumetric tetrahedral grids suitable for numerical simulations (Fig. 2). The data created were then imported into the Gambit 2.2.30 (Fluent, Lebanon, N.H.) software for surface and volume discretization.

Porous medium modelling and CFD

The main objective of this study was to model the endosaccular deployment of the platinum coils with the developing thrombus in the aneurysm volume as a porous medium of decreasing porosity. This idea was based on the uniformity and randomness of the coiling process and the relative scales involved. Moreover, it seems to be the only feasible option—within current and projected computational resources—since it can yield self-consistent numerical results (grid-independent).

Mathematical models describing transport phenomena through porous regions depend on a set of constituent characteristics of the porous medium. The methodology presented here requires the specification of the porosity, inverse permeability and the drag factor for flow through the porous medium. The porosity of the medium represents the volume occupied by the pores to the total volume of the system, while permeability is a measure of the fluid conductivity through the porous medium, representing the surface area to volume ratio of the porous matrix. Our porous media model followed the theory of Kozeny [12] and all changes in porosity, interstitial surface area and permeability during the coiling process (Table 2) were derived following the clinical coil chart (Table 1). The corresponding drag factor in the porous medium was estimated at $C_D \approx 2.2$ [13]. The orthogonal dimensions of the aneurysm were axial 9.4 mm, sagittal 7.8 mm and coronal 11 mm, giving a total volume of $V_{an} = 4.22293 \times 10^{-7} \text{ m}^3$. All the coils used were size 10, having a diameter, d , of $2.54 \times 10^{-4} \text{ m}$. Assuming that blood flow has an average velocity of $V_{av} = 0.1 \text{ m/s}$, the Reynolds number (Re) at the inlet of the vasculature is 213 varying up to 363 close to the aneurysm (flow conditions appropriate to the anterior communicating artery [14]).

Table 1 Coiling procedure for occlusion of our anterior communicating artery aneurysm

Coil	Circular memory (mm)	Diameter (m $\times 10^{-4}$)	Length (m)	Surface (m ² $\times 10^{-5}$)	Volume (m ³ $\times 10^{-9}$)	Packing density
1	10	2.54	0.30	23.9491	15.2012	0.036
2	9	2.54	0.30	23.9491	15.2012	0.072
3	8	2.54	0.30	23.9491	15.2012	0.108
4	8	2.54	0.20	15.9694	10.1341	0.132
5	7	2.54	0.20	15.9694	10.1341	0.156
6	7	2.54	0.10	7.98978	5.06707	0.168
7	6	2.54	0.20	15.9694	10.1341	0.192
8	6	2.54	0.10	7.98978	5.06707	0.204
9	5	2.54	0.15	11.9796	7.60061	0.222
10	5	2.54	0.10	7.98978	5.06707	0.234
11	4	2.54	0.08	6.39385	4.05366	0.244
12	3	2.54	0.06	4.79792	3.04024	0.251
13	3	2.54	0.04	3.20199	2.02683	0.256
14	2	2.54	0.04	3.20199	2.02683	0.260
15	2	2.54	0.04	3.20199	2.02683	0.265

A haemodynamic model was subsequently developed to describe the flow, pressure and force fields of the system. This was implemented on CFD-ACE software (ESI Group, Rungis, France) [15] assuming a Newtonian liquid of density $\rho=1069$ kg/m³ and constant dynamic viscosity $\mu=0.0035$ kg/m-s, nonpulsatile flow, noncompliant walls and constant outlet pressure.

Results

We report the results of computational haemodynamic calculations for three different stages of the coiling procedure: following deployment of the 1st coil, the 7th coil (intermediate stage of the coiling simulation), and the 15th and final coil, leaving a small residual neck remnant. For every simulation, blood flow patterns and velocity as well as wall pressure distribution were computed and compared with the pretreatment simulation.

Introduction of the first coil had a dramatic effect on the blood flow pattern, although it occupied only 3.6% of the

aneurysm volume (porosity 0.964, Tables 1 and 2). This first coil, as represented in the simulation by the porous medium, changed the endosaccular flow pattern from complex vortical to a concentrated inlet/outlet mode with more organized and defined streaming (Fig. 3). Similar changes in blood flow velocity were also detected at this stage (Figs. 4b and 5b).

At an intermediate stage in the coiling simulation, i.e. during deployment of the 7th coil, the aneurysm occlusion was 19.2% and a significant decrease in blood flow velocity was noted with stagnation in some areas (Figs. 4c and 5c). At the end of the coiling simulation, a packing density of 26.5% (represented by a porosity of 0.735 in the porous

Table 2 Porosity characteristics for our anterior communicating artery aneurysm

Coil	Porosity	Interstitial surface area (m ²)	Permeability (m ² $\times 10^{-8}$)
1	0.964	567.119908	144.470
2	0.928	1134.23982	33.4705
3	0.892	1701.3597	13.7441
4	0.868	2079.51966	8.71154
5	0.844	2457.67959	5.89683
6	0.832	2646.87954	4.94042
7	0.808	3025.03947	3.56737
8	0.796	3214.23943	3.06661
9	0.778	3497.91937	2.47361
10	0.766	3687.11933	2.15812
11	0.756	3838.52729	1.94164
12	0.749	3952.14325	1.79691
13	0.744	4027.96722	1.70780
14	0.740	4103.79119	1.62413
15	0.735	4179.61516	1.54548

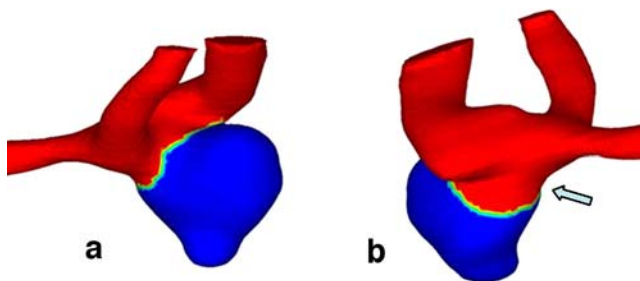


Fig. 2 Aneurysm computer model with partition of its volume into a porous medium (blue) and a pure fluid part (red). Notice also the accommodation of the neck remnant (arrow)

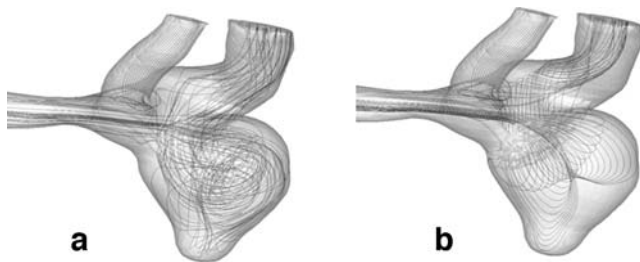
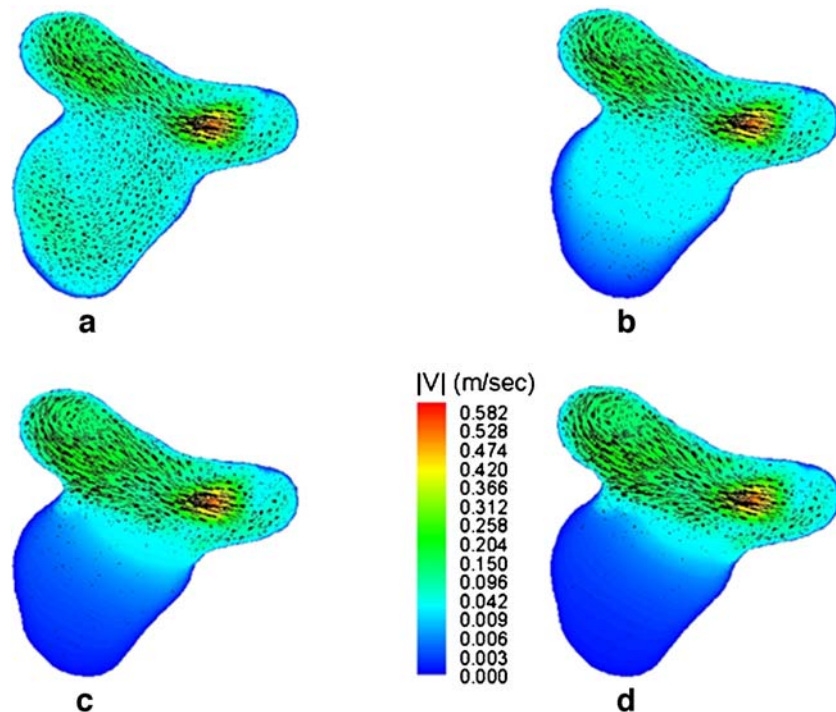


Fig. 3 Flow patterns before (a) and after (b) simulation of the deployment of the first coil. A significant change to a more constructed mode is identified

medium, Tables 1 and 2) was achieved and the decrease in flow velocity was so profound that large areas, especially around the aneurysm dome, showed blood flow arrest and stagnation (Fig. 4d). At the same time, flow was still detected at the coil mesh/parent vessel interface, i.e. at the aneurysm neck area (Fig. 5d). This was despite a simulation of packing density above the average (a mean packing density of 24–25% is suggested as enough for a stable occlusion by most authors) [16, 17].

Although the gradual introduction of coils results in a stepwise relief of wall pressure at the aneurysm dome, a redistribution of wall pressure was identified at the aneurysm inflow zone during the intermediate stage of coil packing. This was also evident at the end-of-treatment simulation (Fig. 6) and may be a factor in determining if aneurysm recurrence and regrowth subsequently occurs.

Fig. 4 Velocity (m/s) contours at a sagittal slice before (a) and after simulation of the deployment of the 1st (b), 7th (c) and 15th (d) coils. A gradual reduction in blood flow velocity up to stagnation is obvious

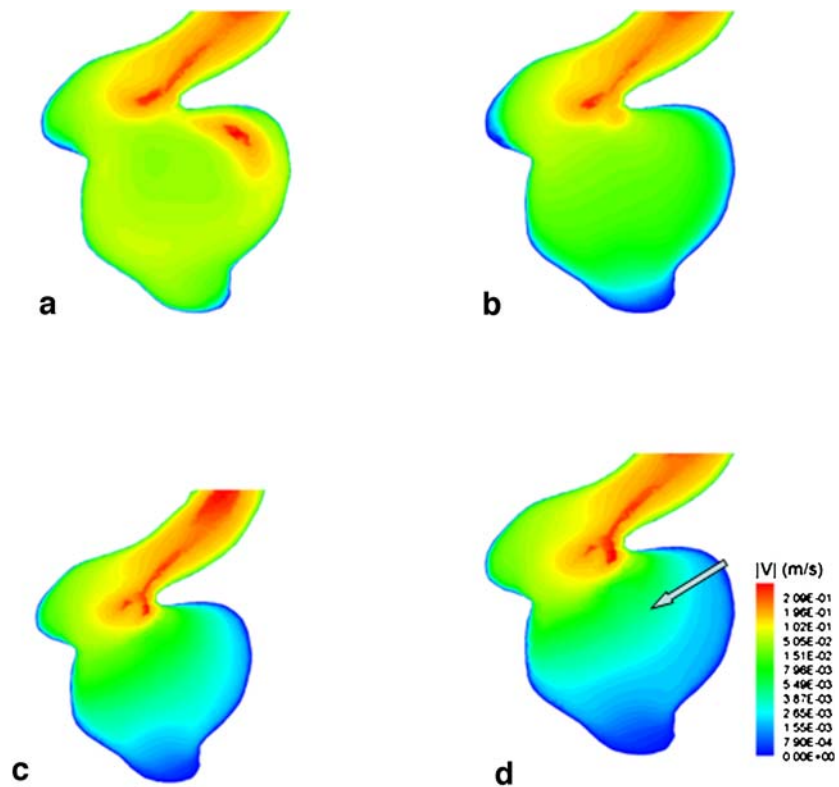


Discussion

The main purpose of this study was to examine whether a porous medium approach, with porous characteristics derived to simulate the coils actually used during treatment, is capable of simulating the haemodynamic consequences of coiling. The porous medium representation of the coil mesh allows the simulation of blood flow circulating through the coil basket during all coiling stages and even after achieving a satisfactory packing density level. This seems to be close to a realistic representation of the *in vivo* situation, in which the coil mesh does not act as a solid barrier but rather obstructs and slows intra-aneurysmal blood flow circulation, to promote blood stagnation and clot formation.

Further validation and encouragement for our modelling approach is derived from observed consistency with clinical observations and practice. Follow-up clinical series [18–22] have consistently shown significant recurrence and/or recanalization rates (17–20%), especially in large wide-necked aneurysms, but low rebleeding rates (0.5–0.8%). The favourable haemodynamic environment created by the coiling process facilitates intraaneurysm thrombosis, protecting the vulnerable aneurysm dome area and preventing rebleeding. However, the redistribution of wall pressure to the neck area and the persistent flow through the coil mesh, especially if a neck remnant coexists, may contribute to the relatively high rate of coil compaction and recanalization.

Fig. 5 Velocity (m/s) contours at a coronal slice before (a) and after simulation of the deployment of the 1st (b), 7th (c) and 15th (d) coils. There is still marked blood flow velocity at the coil mesh interface in the neck area (arrow), even after coiling is completed (d)



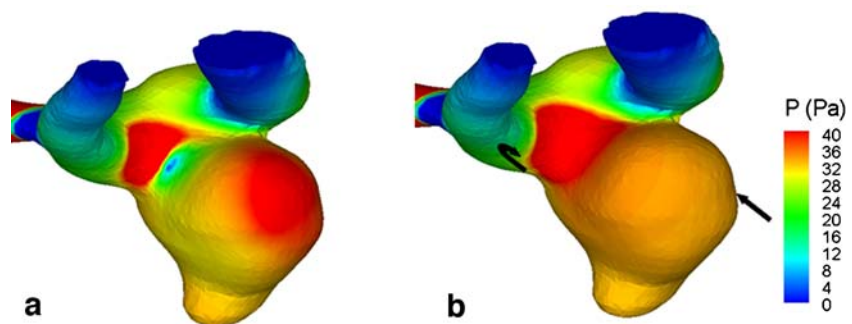
It is obvious though that the complex phenomena of aneurysm thrombosis, recanalization and growth cannot be oversimplified and explained in haemodynamic terms only [23]. Furthermore, we know that the haemodynamic parameters can be seriously affected by many factors such as different aneurysm geometries and local haemodynamic conditions and thus general conclusions cannot be drawn from a single case only.

In the literature there have been attempts to simulate aneurysm coiling using different methods, but obtaining qualitatively similar results to ours. Byun and Rhee [24] reported CFD calculations for artificially constructed models focusing on different parent vessel geometries and coil placement assuming coils to be a sphere of blocked cells.

Groden et al. [25] also employed an artificial CFD model using blocked cells to represent individual coils. Our methodology, based on porous media, follows a randomized process of coil simulation in the aneurysm lumen, eliminating the uncertainty introduced by the level of local grid refinement around individual coils and is therefore computationally efficient and self-consistent, since it leads to grid-independent solutions.

Most modelling attempts to simulate clinical situations—including the one described here—suffer from simplifying assumptions such as rigid walled vasculature, blood being considered as a Newtonian fluid, and use of steady-state blood flow. We adopted the last compromise in order to reduce the computational effort required for the simulations

Fig. 6 Wall pressure (Pa) contours before (a) and after (b) coiling simulation. Although the high pressure at the aneurysm dome has been relieved (b straight arrow), an extension of the high pressure area to the neck remnant is also noted (b curved arrow)



since the aim of the study was to test the utilization of the porous medium representation of the coil complex. However, our team has performed further additional simulations using the same method with different aneurysm geometries, porous media parameters and blood flow velocities, which resulted in similar haemodynamic alterations, enhancing further our confidence in the reliability of the proposed method.

By simulating a coiling scenario for a particular aneurysm, we obtained an overview of the haemodynamics in order to test the feasibility of porous media as a means for modelling coils in CFD. The use of porous media in this context is the novelty of this study and this method has not been used previously. The results of the simulations are encouraging and we plan to continue with further CFD studies using this technique. These will include induction of pulsatile flow, in addition to steady flow, as well as a series of aneurysm models based on different clinical cases. Furthermore, additional developments regarding the simulation of the coagulation process are also in progress by our team [26], which will further enhance the reliability of the modelling approach.

Conclusion

This study demonstrates that a computational simulation technique applied to patient-specific aneurysm geometry can be used to model the haemodynamic consequences of coiling. Although it seems that porous media may be a promising method for simulating coiling in such CFD models, it is obvious that there is a long way to go before simulations can be used as a basis for clinical decisions. However, it seems likely that in the future simulation studies will become a valuable tool in interventional treatment planning and decision-making.

Conflict of interest statement We declare that we have no conflict of interest.

References

- Butty VD, Gudjonsson K, Buchel P, Makhijani VB, Ventikos Y, Poulidakos D (2002) Residence times and basins of attraction for a realistic right internal carotid artery with two aneurysms. *Biorheology* 39:387–393
- Steinman DA, Milner JS, Norley CJ, Lownie SP, Holdsworth DW (2003) Image-based computational simulation of flow-dynamics in a giant intracranial aneurysm. *AJNR Am J Neuroradiol* 24:559–566
- Castro MA, Putman CM, Cebal JR (2006) Patient-specific computational modelling of cerebral aneurysms with multiple avenues of flow from 3D rotational angiography images. *Acad Radiol* 13:811–821
- Burleson AC, Strother CM, Turitto VT (1995) Computer modelling of intracranial saccular and lateral aneurysms and the study of their haemodynamics. *AJNR Am J Neuroradiol* 37:774–784
- Cebal JR, Castro MA, Burgess JE, Pergolizzi RS, Sheridan MJ, Putman CM (2005) Characterization of cerebral aneurysms for assessing risk of rupture by using patient-specific computational hemodynamics models. *AJNR Am J Neuroradiol* 26:2550–2559
- Jou LD, Wong G, Dispensa B, Lawton MT, Higashida RT, Young WL, Saloner D (2005) Correlation between luminal geometry changes and haemodynamics in fusiform intracranial aneurysms. *AJNR Am J Neuroradiol* 26:2357–2363
- Shojima M, Oshima M, Takagi K, Torii R, Hayakawa M, Katada K, Morita A, Kirino T (2004) Magnitude and role of wall shear stress on cerebral aneurysm: computational fluid dynamic study of 20 middle cerebral artery aneurysms. *Stroke* 35:2500–2505
- Acevedo-Bolton G, Jou L-D, Dispensa BP, Lawton MT, Higashida RT, Martin AJ, Young WL, Saloner D (2006) Estimating the haemodynamic impact of interventional treatments of aneurysms: numerical simulation with experimental validation: technical case report. *Neurosurgery* 59:E429–E430
- Aenis M, Stancampiano AP, Wakhloo AK, Lieber BB (1997) Modeling of flow in a straight stented and nonstented side wall aneurysm model. *J Biomech Eng* 119:206–212
- Jou LD, Quick CM, Young WL, Lawton MT, Higashida R, Martin A, Saloner D (2003) Computational approach to quantifying haemodynamic forces in giant cerebral aneurysms. *AJNR Am J Neuroradiol* 24:1804–1810
- Hassan T, Ezura M, Timofeev EV, Tominaga T, Saito T, Takahashi A, Takayama K, Yoshimoto T (2004) Computational simulation of therapeutic parent artery occlusion to treat giant vertebrobasilar aneurysm. *AJNR Am J Neuroradiol* 25:63–68
- Koponen A, Kataja M, Timonen J (1997) Permeability and effective porosity of porous media. *Phys Rev E* 56:3319–3325
- Achenbach E (1971) Influence of surface roughness on the cross-flow around a circular cylinder. *J Fluid Mech* 46:321–335
- Ujiie H, Liepsch DW, Goetz M, Yamaguchi R, Yonetani H, Takakura K (1996) Hemodynamic study of the anterior communicating artery. *Stroke* 27:2086–2094
- ESI Group (2006) CFD-ACE users manual. ESI Group Huntsville, AL
- Piotin M, Mandai S, Kieran J, Sugi K et al (2000) Dense packing of cerebral aneurysms: an in vitro study with detachable platinum coils. *AJNR Am J Neuroradiol* 21:757–760
- Kawanabe Y, Sadato A, Taki W, Hashimoto N (2001) Endovascular occlusion of intracranial aneurysms with Guglielmi detachable coils: correlation between coil packing density and coil compaction. *Acta Neurochir (Wien)* 143:451–455
- Byrne JV, Sohn MJ, Molyneux AJ, Chir B (1999) Five-year experience in using coil embolization for ruptured intracranial aneurysms: outcomes and incidence of late rebleeding. *J Neurosurg* 90:656–663
- Cognard C, Weill A, Spelle L, Piotin M, Castaing L, Rey A, Moret J (1999) Long-term angiographic follow-up of 169 intracranial berry aneurysms occluded with detachable coils. *Radiology* 212:348–356
- Raymond J, Guilbert F, Weill A, Georganos S, Juravsky L, Lambert A, Lamoureux J, Chagnon M, Daniel Roy D (2003) Long-term angiographic recurrences after selective endovascular treatment of aneurysms with detachable coils. *Stroke* 34:1398–1403
- Murayama Y, Nien YL, Duckwiler G, Gobin YP, Jahan R, Frazee J, Martin N, Vinuela F (2003) Guglielmi detachable coil embolization of cerebral aneurysms: 11 years' experience. *J Neurosurg* 98:959–966
- Vinuela F, Duckwiler G, Maward M (1997) Guglielmi detachable coil embolization of acute intracranial aneurysms: perioperative anatomical and clinical outcome in 403 patients. *Neurosurg* 86:475–482
- Horowitz MB, Purdy PD, Burns D, Belloto D (1997) Scanning electron microscopic findings in a basilar tip aneurysm embolized

- with Guglielmi detachable coils. *AJNR Am J Neuroradiol* 18:688–690
24. Byun HS, Rhee K (2004) CFD modelling of blood flow following embolisation of aneurysms. *Med Eng Phys* 26:755–761
 25. Groden C, Laudan J, Gatchell S, Zeumer H (2001) Three-dimensional pulsatile flow simulation before and after endovascular coil embolization of a terminal cerebral aneurysm. *Cereb Blood Flow Metab* 21:1464–1471
 26. Bedekar AS, Pant K, Ventikos Y, Sundaram S (2005) A computational model combining vascular biology and haemodynamics for thrombosis prediction in anatomically accurate cerebral aneurysms. *Food Bioprod Process* 83(C2):118–126